Physicochem. Probl. Miner. Process., 60(2), 2024, 187844

http://www.journalssystem.com/ppmp

Physicochemical Problems of Mineral Processing

ISSN 1643-1049

Effect of the type of ion-exchange resin on Mn^{2+} adsorption in the presence of competing cations

Bruna P. C. Amengol [1], Renata. C. Pires [2], Versiane Albis Leão [3]

[1] Universidade Federal de Ouro Preto, Graduate Program in Environmental Engineering, Campus Morro do Cruzeiro, s.n., Bauxita, Ouro Preto, MG, 35400-000, Brazil. rr

[2] Universidade Federal de Ouro Preto, Hydrometallurgy Laboratory, Department of Metallurgical and Materials Engineering (re_cpires@yahoo.com.br). Campus Morro do Cruzeiro, s.n., Bauxita, Ouro Preto, MG, 35400-000, Brazil.

[3] Universidade Federal de Ouro Preto, Hydrometallurgy Laboratory, Department of Metallurgical and Materials Engineering (versiane@ufop.edu.br). Campus Morro do Cruzeiro, s.n., Bauxita, Ouro Preto, MG, 35400-000, Brazil.

Corresponding author: versiane@ufop.edu.br (Versiane Leão)

Abstract: Present in soils, ground and surface waters, manganese is among the most common metals in Earth crust. It is also an essential trace element to the functioning of several enzymes in the human body. However, exposure to high manganese concentrations can also be harmful to humans with psychiatric and motor effects and therefore, manganese concentrations in drinking water and also industrial effluents are regulated. In the current work, the adsorption of Ca^{2+}, Mg^{2+} and Mn^{2+} on three different ion-exchange resins: (i) aminophosphonic acid - chelating (Purolite S950), (ii) polyacrylic weak acid cation (Purolite C104E) and (iii) polystyrene strong acid cation (Purolite C100) was investigated. The results revealed that Purolite S950 had the highest Mn^{2+} uptake (37.9 mg/mL-resin or 0.69 mmol/mL-resin) as compared to Ca^{2+} (3.2 mg/mL-resin or 0.08 mmol/mL-resin) and Mg^{2+} (~0 mg/mL-resin) and was selected for further kinetics and equilibrium studies. The results indicated Purolite S950 as particularly suited to be applied in the treatment of neutral mine waters with high Mg/Mn ratios. Additionally, Purolite S950 showed a small affinity for Ca^{2+} and therefore an efficient Mn^{2+} removal will depend on the Ca/Mn ratio of the mine water under treatment. According to the kinetic analysis, manganese sorption on Purolite S950 was described by the pseudo-second order model ($r^2 > 0.98$) with an activation energy of 10.40 kJ/mol and thus pore-difussion was the rate controlling step of the process. In terms of equilibrium studies, manganese sorption on Purolite S950 followed the Langmuir model with maximum loadings of up to 41.5 mg/mL-resin. The thermodynamic modelling indicated an exothermic process (-85.0 kJ/mol, as standard enthalpy) with a standard entropy of -274 J/mol·K, which was ascribed to the release of two adsorbed H^+ ions for each Mn^{2+} ion taken up from solution

***Keywords*:** manganese, chelating resin, mine waters, selectivity, activation energy

1. Introduction

Mining stands as a crucial industrial activity, particularly in developing nations across South America and Africa. With the depletion of high-grade deposits globally, the focus has shifted to processing lower-grade ores. Various concentration techniques are employed to increase the content of the valuable mineral in the final product. However, this process generates immense volumes of waste, reaching an around 14 billion tonnes worldwide in 2010 (Adiansyah et al., 2015). Typically, these tailings are deposited into ponds, some of which rank among the largest man-made structures. Consequently, addressing the substantial challenges linked to mitigating the risks associated with potential dam failures becomes paramount.

Regrettably, failures of tailing dams are not uncommon within the mining sector. Notable instances include the Philex Padcal gold mine in the Philippines (2012), the dam breach at the Mount Polley gold-copper mine in Canada (2014), and the incident at the Cadia gold mine in Australia (2018) (Owen et al., 2020). While these non-ferrous operations may not rank among the largest in the mining industry, the

DOI: 10.37190/ppmp/187844

impact of the failure on the quality of receiving waters can be severe due to acidity and the presence of toxic metals such as As, Cd and Pb.

Iron ore production represents a prime example of large-scale mining operations, producing approximately 2.5 billion tons in 2019 (Tuck, 2020). The demand for iron ore stems from its pivotal role as a raw material in the iron and steel production—a technology pioneered during the industrial revolution. With abundant reserves available, the iron and steel industry can be efficiently scaled to meet the substantial needs of various infrastructure projects, including housing, railways, and automobile production. The production centres for iron and steel are primarily concentrated in Asia, with Brazil and Australia serving as major iron ore providers. While numerous iron ore mines in Australia are located in sparsely populated regions, Brazilian operations are notably concentrated in the states of Minas Gerais and Pará. Minas Gerais, in particular, holds historical significance as the birthplace of Brazil's iron industry and ranks second in population density, housing several operations close to densely populated areas. Consequently, the occurrence of two dam failures in this state had catastrophic consequences, impacting both the economy and the environment.

In November 2015, a catastrophic failure occurred at the Fundão tailings dam in the Germano iron ore mine (operated by Samarco/Vale/BHP) in Mariana. Approximately 34 million cubic meters of ore tailings and residues were released, reaching the Gualaxo do Norte River within the Rio Doce basin and causing the dispersal of various toxic metals into these rivers. Notably, manganese has shown enduring effects on water quality .Specifically, the total manganese concentration peaked at 936mg/L immediately after the accident (Instituto Mineiro De Gestão Das Águas, 2015). In the subsequent years, the manganese concentration progressively reduced but the manganese content in the river waters increases whenever the wet season (summer) is particularly intense, suggesting that the mining tailings deposited in the riverbed releases manganese to the water column (Instituto Mineiro De Gestão Das Águas, 2020).

Although the aquatic chemistry of manganese is complex, the element is mostly found as the Mn^{2+} ion because this species is very stable in aqueous solutions. The stability of Mn^{2+} ion is greater in acid and neutral environments and decreases as the pH is raised before it is precipitated as $Mn(OH)_2$. Precipitating Mn^{2+} as hydroxide may be an option to remove manganese, but the alkalis consumption is often considered high, given the pH required to reduce the Mn^{2+} concentrations to the value defined in specific environmental regulations (Barboza et al., 2016).

The oxidation of Mn^{2+} and its precipitation as oxides (MnO_2, Mn_3O_4 and Mn_2O_3) can also be a strategy to remove manganese from mining-affected waters. However, the oxidation potential required for such precipitation is quite high and the oxidation kinetics is very slow (Morgan, 2005) at pH values below 8. As the pH is increased, the potential required to produce solid manganese oxides is decreased and oxygen becomes able to oxide Mn^{2+} to Mn^{4+} (Barboza et al., 2016). Another positive effect of removing manganese in alkaline pH is the fact that the kinetics of Mn^{2+} oxidation by oxygen is catalysed when the pH is increased.

Several strategies have been proposed to address the issue of manganese removal from mine affected waters, but a standard, well accepted solution is yet to be adopted. The widespread practice in several countries is to apply lime to increase the pH and precipitate the metals present in mine waters as hydroxides. However, an efficient removal of Mn^{2+} ions requires a pH above 9.0 - a value that does not enable the direct release of the final effluent in several countries. In addition, excessive lime consumption is required to reach such pH values. Therefore, different approaches for the removal of Mn^{2+} ions are necessary and the current work selected adsorption to treat manganese-laden waters. Therefore, the current research investigated the selection of a ion exchange resin to adsorb Mn^{2+} in the presence of Ca^{2+} and Mg^{2+} ions and the kinetics and equilibrium analysis of such adsorption.

2. Materials and methods

2.1. Ion exchange resins

Manganese adsorption on three ion-exchange resins were investigated in the current work i. e. Purolite C100 (strong acid cation), Purolite C104E (weak acid cation) and Purolite S950 (aminophosphonic acid chelating). The main features of each resin are listed in Table 1.

Prior to the sorption experiments, all resins were pre-prepared following specific procedures. In this regard, 1mol/L NaOH solutions were used to convert Purolite C104E resin to Na-form. Furthermore, Purolite C100 and Purolite S950 were conditioned with distilled water and an acidified aqueous solution (pH 3.5), respectively, for the same purpose.

Table 1. Features of Purolite C100, C104E and S950 ion exchange resins

Resin	**Purolite C100**	**Purolite C104E**	**Purolite S950**
Matrix	polystyrene	Polyacrylic	Polystyrene
Exchange group	Sulfonic acid	Carboxylic acid	amino-phosphonic
Total exchange capacity (min)	2.0 eq/L	3.8 eq/L	1.2 eg/L Ca
Operation range (pH)	0-14	5-14	2-6 (H^+) - 6-11 (Na)
Maximum working temperature	120°C	120°C	90°C

2.2. Solution preparation

Firstly, a mono-element solution was prepared from $MnSO_4.H_2O$ (99%) and distilled water in which the Mn^{2+} concentration was set at 500 mg·L^{-1} (9.1 mmol·L^{-1}) and the pH was adjusted to 4.5, using sulphuric acid. Moreover, a multimetallic solution was prepared for the selectivity studies using calcium chloride ($CaCl_2{\cdot}2H_2O$, 99%) magnesium chloride ($MgCl_2{\cdot}6H_2O$, 99.04%), along with manganese sulphate ($MnSO_4{\cdot}H_2O$, 99%). The concentration of each metal was 12 mmol/L, which corresponds to 659.2 mg/L Mn^{2+}, 480.9 mg/L Ca^{2+} and 291.7 mg/L Mg^{2+} and the pH was also 4.5.

2.3. Manganese adsorption and selectivity with regard to calcium and magnesium

The selectivity of the three resins for manganese (Mn^{2+}) in relation to Ca^{2+} and Mg^{2+} was determined using a solution containing 12 mmol·L^{-1} of each ion (659.2 mg/L Mn^{2+}, 480.9 mg/L Ca^{2+} and 291.7 mg/L Mg^{2+}), at pH 4.5. The procedure comprised transferring 1 mL of each resin and 100 mL of the three-metal solution to a 250 mL-flask, which was then placed in temperature-controlled shaker (*New Brunswick Scientific*, "*INNOVA 44*"). This equipment was carried out at 25°C and 130 min^{-1} as the stirring rate. Seven sequential resin loadings with each sorption cycle during 10 hours had the aim of approaching resin saturation with the three metallic ions. At the end of the experiment the solution-resin pulp was filtered and the aqueous phase was sent to chemical analysis in an ICP-OES (*Agilent - 725 ES*). Subsequently, the resin loading (q), was determined by a mass balance as either mg Metal/mL-resin or mmol Metal/mL-resin. Duplicate experiments were carried out in this step.

2.4. Kinetics studies

In the kinetics study, the experiments were carried out batchwise in a closed water-jacket borosilicate glass reactor (SCHOTT DURAN) with 600mL as the total volume. Stirring was provided by a glass rod connected to an IKA RW 20 overhead stirrer. Hot water was pumped throughout the glass reactor by a water bath (Ultratermostato Criostato modelo 521D - Nova Ética) for temperature control. All tests were carried out by mixing 5 mL of Purolite S950 resin with 500 mL of $MnSO_4$ solutions containing 350 mg/L Mn^{2+} (as $MnSO_4$). The experiments lasted up to 6 h and 3 mL-samples were collected every 5 minutes in the first half-hour. Subsequently samples were withdrawn at every 10 min (or 15 min), before being sent to chemical analysis in an ICP-OES (Agilent 725) whereas the manganese concentration in the solid phase was determined by mass balance. The effect of the stirring rate was assessed at the range 345 min^{-1} - 720 min^{-1} in order to determine the value from which film diffusion no longer affected the sorption kinetics. Moreover, the effect of temperature was studied in the 40°C-70°C range. By fitting to pseudo-second order model (Eq. 1) to the resin loadings as a function of time t (q_t), the rate constant k_2 at each temperature was determined. Subsequently, the activation energy was calculated using the rate constant values, by applying the Arrhenius equation (Eq. 2).

$$q_t = \frac{k_2 {q_\infty}^2 t}{1 + k_2 q_\infty t} \quad (1)$$

$$k_2 = k_0 . \exp\left(-\frac{E_a}{RT}\right) \quad (2)$$

In Eq. 1 and Eq. 2, q_∞ is an adjustable parameter, k_2 is the rate constant and t is time; k_0 is the frequency factor; T is the temperature (K), Ea is the activation energy (J/mol) and R is the universal gas constant (8.314 J/mol.K).

2.5. Equilibrium studies

The procedure applied in the equilibrium studies consisted of mixing 1 mL of Purolite S950 resin with 100 mL of a manganese sulphate solution containing from 50 mg·L^{-1} to 120 mg/L Mn^{2+}, at pH 4.5. All sorption experiments were performed in a New Brunswick Scientific "INNOVA 44" shaker until equilibrium was attained, at different temperatures. After 24h (at least) of testing, the loaded resin was separated from the solution by filtration. The initial and final samples had their manganese concentrations determined by ICP-OES and the resin loadings (as mgMn^{2+}/mL-resin) were determined by mass balance. Values of the resin loading (q_{eq}) and solution concentrations at equilibrium (C_{eq}) were described by the Langmuir equation (Eq. 3), where q_{max} is the maximum sorption capacity and b is the Langmuir constant.

$$q_{eq} = \frac{q_{max} b C_{eq}}{1 + b C_{eq}} \quad (3)$$

Similarly, the effect of temperature on the equilibrium sorption was assessed by applying the van't Hoff equation (Karthikeyan *et al.*, 2005; Wu *et al.*, 2009), whereby both standard enthalpy of sorption (ΔH^0) and standard entropy (ΔS^0) of sorption were estimated based on the equilibrium constant (*b* from the Langmuir isotherm*)* at different temperatures (T).

$$\ln(b) = \frac{\Delta H^0}{RT} + \frac{\Delta S^0}{R} \quad (4)$$

3. Results and discussion

3.1. Resin selectivity for Mn^{2+} ions in the presence of Ca^{2+} and Mg^{2+}

Irrespective of the type of adsorbent applied in the removal of toxic metals from wastewaters, it is always relevant to address resin selectivity for the target ion in relation to other aqueous species found in these wastewaters. This is because the selectivity of ion exchange resins is affected by different factors such as charge and concentration. In this regard, investigating resin selectivity for alkaline-earth and transition metal ions is relevant for the current study. As the exchange group in the resin defines affinity for metals, manganese loading in the presence of the same molar concentration of both Ca^{2+} and Mg^{2+} ions by three different resins (Purolite C100 - strong acid cation; Purolite C104E - weak acid cation and Purolite S950 - aminophosphonic acid chelating) was investigated (Fig. 1) The solution used in these experiments was composed of 659.2 mg/L Mn^{2+}, 480.9 mg/L Ca^{2+} and 291.7 mg/L Mg^{2+}, i. e. 12 mmol/L of each cation. The ions Ca^{2+} and Mg^{2+} were included as examples as their concentrations can be much higher than that of manganese. Calcium concentrations around 400mg/L are usually determined in neutral mine waters, particularly when lime is used to remove acidity. Conversely, the magnesium content can vary extensively, from a few milligrams per litre to values over 1g/L, depending on the mineralogy of the mine (Heikkinen *et al.*, 2009; Sracek *et al.*, 2011).

According to Fig. 1, the aminophosphonic acid chelating resin Purolite S950 showed the highest Mn^{2+} uptake, i. e. 37.9 mg/mL-resin (0.69 mmol/mL-resin) as compared to the alkaline-earth ions i. e. 3.2 mg/mL-resin Ca^{2+} (0.08 mmol/mL-resin) and ~0 mg/mL-resin Mg^{2+}. A similar outcome was observed in the case of the weak acid resin (Purolite C104E cation), although the 22.5 mg/mL-resin (0.41 mmol/mL-resin) Mn^{2+} loading was smaller than that observed in Purolite S950. Fig.1 also depicts the three ions adsorption on the strong acid cation Purolite C100 resin. In the latter, the highest loading 24.8 mg/mL-resin (0.62 mol/mL-resin) was achieved in the case of calcium, followed by 9.3 mg/mL-resin (0.17 mmol/mL-resin) manganese and 3.4 mg/mL-resin (0.14 mmol/mL-resin) magnesium. Therefore, both Purolite S950 and C104E resins presented the highest selectivity for manganese as compared to calcium and magnesium. However, Purolite S950 had the highest Mn^{2+} uptake among the three resins and was selected for further studies. The adsorption of different metals on Purolite S950 in the context of nickel recovery from laterite ores showed only the uptake of copper, manganese,

magnesium and zinc from a solution also containing aluminium, cobalt, chromium, iron and nickel. The resin presented stronger affinities for Cu^{2+}, Zn^{2+} and Mn^{2+} followed by Mg^{2+} (Perez *et al.*, 2018), which is similar to the affinity series proposed by Hamabe et al. (2009) for the adsorption of divalent cations (Ni^{2+}<Ca^{2+}<Mg^{2+}< Zn^{2+}<Cu^{2+}<Pb^{2+}) on a phosphonate adsorbent. Both studies confirm the low affinity of aminophosphonic chelating resins for Ca^{2+} and Mg^{2+} as compared to transition metals, as expected.

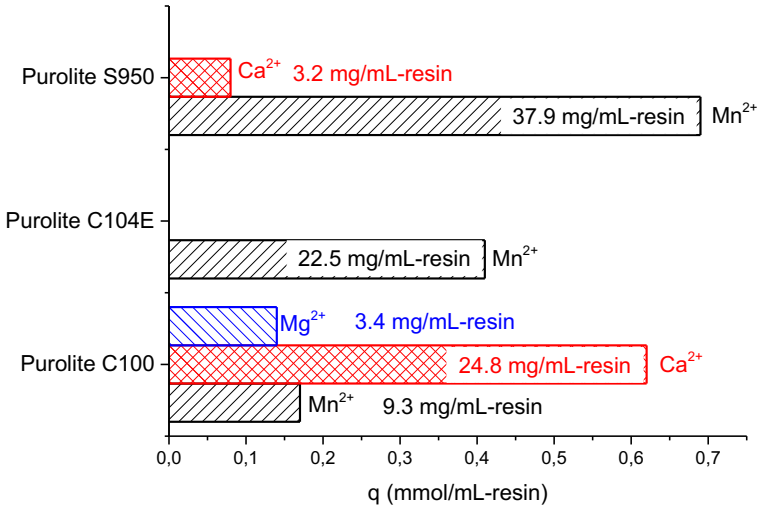

Fig. 1. Mn^{2+}, Ca^{2+}, Mg^{2+} loadings on Purolite S950 (aminophosphonic acid chelating), C104E (carboxilic acid cation) and C100 (sulphonic acid cation), 25°C, 130 min^{-1}; 100 mL of solution containing 12 mmol·L^{-1} (659.2 mg/L Mn^{2+}, 480.9 mg/L Ca^{2+} and 291.7 mg/L Mg^{2+}) of each species, at pH 4.5 mixed with 1mL of each resin

A previous study (Amengol, 2021) defined the experimental conditions in which the highest Mn^{2+} loadings on Purolite S950 were achieved, both in terms of concentration (which varied between 150 mg/L Mn^{2+} and 450 mg/L Mn^{2+}) and stirring rate (varied from 345 min^{-1} to 645 min^{-1}). Firstly, it was revealed that applying solutions containing 350 mg/L Mn^{2+} or higher concentrations resulted in resin saturation with manganese at 30 mg/mL-resin, under the experimental conditions applied. In addition, the resin loading was independent of the stirring rate in the entire range investigated, implying that mass transfer through the Nernst boundary layer was not the rate-controlling step (Levenspiel, 1962).

3.2. Kinetic analysis

The kinetic parameters associated to Mn^{2+} adsorption on Purolite S950 were assessed batchwise, by using synthetic manganese sulphate (350 mg/L Mn^{2+}) solutions at different temperatures (40°C to 70°C). The kinetics models tested to describe the solid loadings as a function of time (Fig. 2) were the pseudo-first order and pseudo-second order equations. Such equations are extensively used in adsorption experiments and their formulation can be found in several publications (Gemici et al., 2021; Marcu et al., 2021; Nazarian et al., 2021). Moreover, these two equations consider the sorption process as a whole, without any distinction regarding the rate-controlling step. As mass transfer through the Nernst boundary layer was not the rate-controlling step (Levenspiel, 1962), the effect of temperature on the sorption kinetics was assessed in order to calculate the activation energy of Mn^{2+} adsorption on Purolite S950 and to hypothesize the adsorption mechanism, which could be either pore-diffusion or ion-exchange itself.

To calculate the activation energy (E_a) firstly it is required the determination of the rate-constant (k) at each temperature. Similarly to most studies, the pseudo-second order equation (r^2>0.98) described better the kinetics of manganese adsorption (Fig. 3) as compared to the pseudo-first order model (r^2<0.95). Table 1 lists the rate constant values (k_2) achieved in the current work, which increased from 1.2x10^{-3} g/mg·min at 40°C to 1.7x10^{-3} g/mg·min, at 70°C. This set of values is within the range of values reported when the pseudo-second order equation described metal ion adsorption on ion exchange resins, which vary from 10^{-3} g/mg·min to 10^{-1} g/mg·min.

The Arrhenius equation was applied to determine the value of activation energy (E_a) from the rate constant (k_2) data obtained at each temperature, listed in Table 2. This approach resulted in an activation energy value of 10.40 kJ/mol (Fig. 3).

As film-diffusion was not relevant under the experimental conditions of the current work, the value of activation energy (10.40kJ/mol) indicated that the rate-determining step of Mn^{2+} adsorption on Purolite S950 was pore-diffusion. Manganese sorption on a cation-exchange resin (Sinco-430) was also modelled using the second-order equation and an activation energy of 6.34 kJ/mol was reported, which also suggests pore-diffusion control (Zhuang et al., 2020). Similarly, manganese adsorption on a spent zeolite was also described by the pseudo-second order equation and the activation energy was 55.6 kJ/mol, which can be also ascribed to pore-diffusion control (Figueiredo et al., 2018).

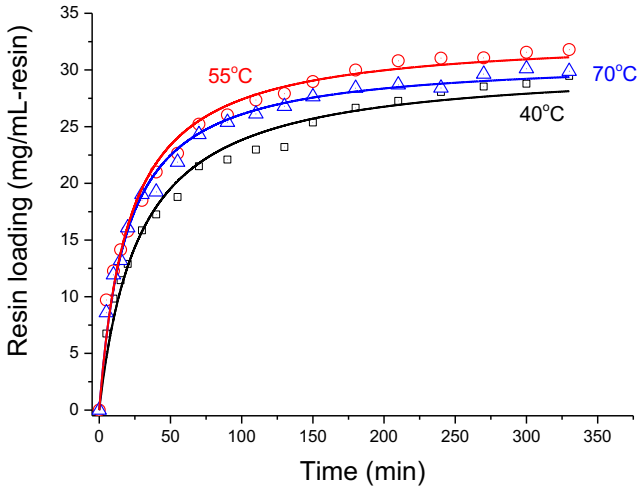

Fig. 2. Fitting of the pseudo-second-order model to the experimental data describing Mn^{2+} adsorption on Purolite S950. Experimental conditions: 500mL of solution containing 350mg/L Mn^{2+}; 5mL of resin; pH 4.5

Table 2. Parameters related to fitting the pseudo-second order equation to Mn^{2+} adsorption on Purolite S950, at different temperatures. Experimental conditions: 500mL of solution containing 350mg/L Mn^{2+}; 5mL of resin; pH = 4.5

Parameter	40°C	55°C	70°C
q_∞ (mg/mL)	30.53	33.08	31.09
k (mL/mg.min)	0.0012	0.0015	0.0017
r^2	0.981	0.985	0.989

3.3. Equilibrium studies

Adsorption equilibrium is represented by isotherms, which indicate the relationship between metal concentrations in the liquid phase and in the adsorbent at constant temperature, at equilibrium (Mccabe et al., 2005). Therefore, the isotherms describing Mn^{2+} adsorption on Purolite S950, at pH 4.5 and at 38.5°C, 50°C and 70°C are shown in Fig. 4.

The Langmuir and Freundlich equations were selected to model the isotherms of Fig. 4. The analysis revealed that the Langmuir equation presented a better fit to the experimental data, as it produced the highest values of the coefficients of determination ($r^2 \geq 0.95$) as compared to the values observed by applying the Freundlich equation ($r^2 \leq 0.92$), Table 3. When an isotherm is described by the Langmuir model adsorption it is assumed to occur in monolayers with all available sites on the surface of the adsorbent occupied homogeneously. From the Langmuir equation, the parameters q_{max} and b were determined, which are, respectively, the maximum loading at equilibrium and a constant related to the affinity between the resin and manganese ions (Table 3). Whereas the maximum loading oscillated between 37.9mg/mL-resin and 41.5mg/mL-resin, the b constant clearly decreased from 0.766L/mg, at 38.5°C to 0.039L/mg, at 70°C. Similarly, the Langmuir equation was also reported to describe Mn^{2+} adsorption on both Lewatit TP 260 resin (q_{max} = 128.3 mg/g-resin; b = 0.22 L/mg), and on bone char (q_{max} = 22.0 mg/g-char; b = 0.47 L/mg) (Coşkun et al., 2016; Sicupira et al., 2014).

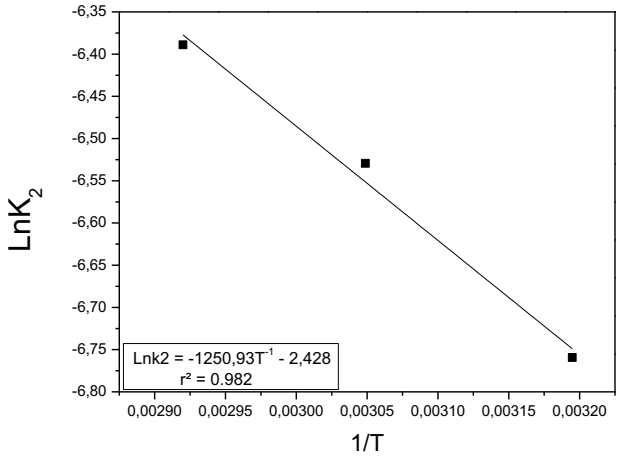

Fig. 3. Arrhenius plot for Mn^{2+} adsorption on Purolite S950. Experimental conditions: Experimental conditions 500mL of a 350mg/L Mn^{2+} solution; 5mL of resin and pH 4.5

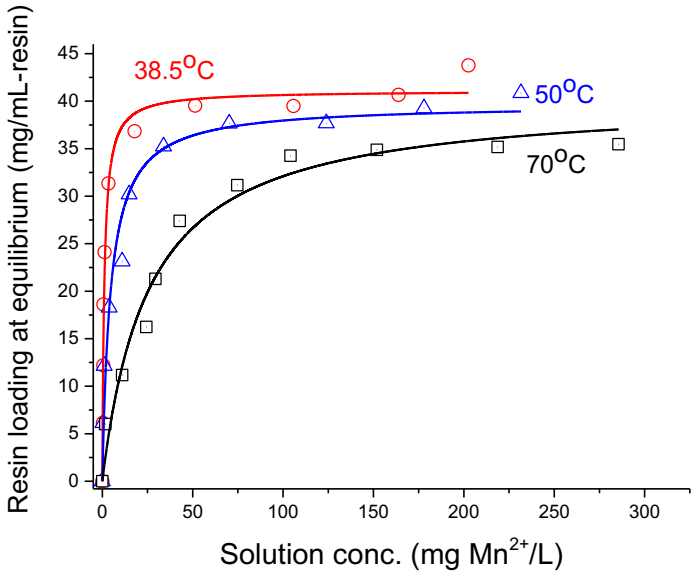

Fig. 4. Adsorption isotherms describing Mn^{2+} adsportion on Purolite S950 at 38.5°C, 50°C and 70°C and fitting to the Langmuir equation. Experimental condition: pH 4.5, 24 hours of testing time

Table 3. Parameters determined by fitting the Langmuir equation to Mn^{2+} adsorption on Purolite S950 at different temperatures and pH 4.5

Parameter	38.5°C	50°C	70°C
q_{max} (mg/mL)	41.49	37.92	40.18
b (L/mg)	0.766	0.309	0.039
r^2	0.954	0.948	0.948

Applying the van't Hoff equation (Eq. 4), the standard ΔH^o and ΔS^o values were determined (Table 3), through a lnb x 1/T diagram (Fig. 5). From Fig. 5, the standard enthalpy and entropy of adsorption were determined as -85.0 kJ/mol and -274 J/mol·K, respectively. Therefore Mn^{2+} adsorption on Purolite S950 was an exothermic process, which was also observed during Mn^{2+} ion adsorption on graphene oxide, which was also exothermic (ΔH^o = -8.08kJ/mol) (Suddai et al., 2017). Conversely, positive ΔH^o values for manganese adsorption in a styrene-divinylbenzene nanocomposite (ΔH^o = 23.69kJ/mol) (Hadadi, 2020) and in anthracite (ΔH^o = +0.23kJ/mol) (El-Aassar and Mohamed, 2021) were reported. Furthermore, the negative value of the standard entropy (-274J/mol·K) implies in a decrease of the number of degrees of freedom of the system as Mn^{2+} ions were adsorbed on the exchange sites of the

resin. However, the total change in entropy (system and surroundings) should be always positive in spontaneous processes and the increase in randomness in the current work may be ascribed to the exchange reaction itself as two H^+ ions are released for each Mn^{2+} ion adsorbed on the resin (Fig 6).

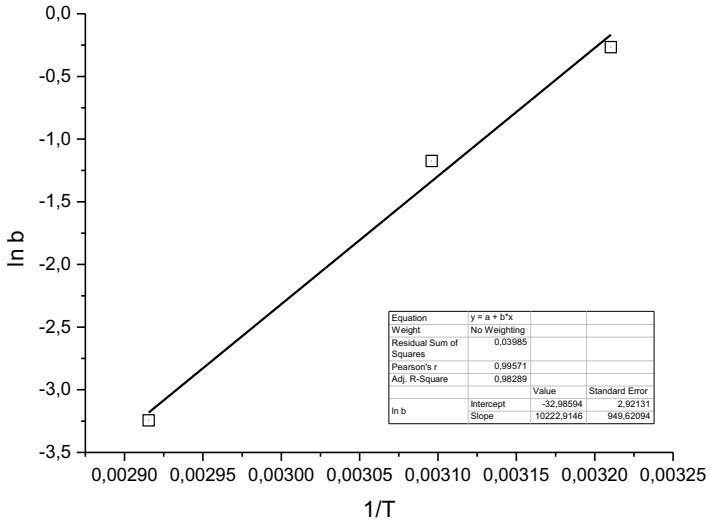

Fig. 5. Van't Hoff diagram for Mn^{2+} adsorption on Purolite S950

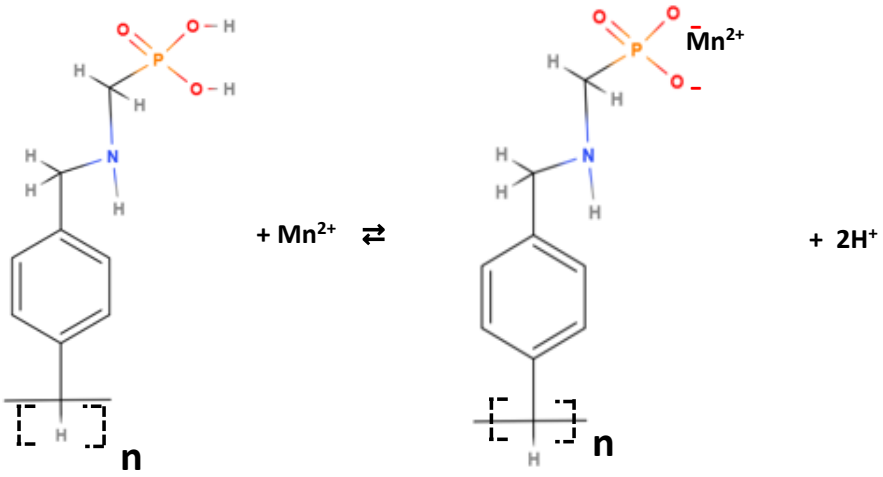

Fig. 6. Ion exchange process in the case of an amino-methyl-phosphonic acid resin (Purolite S950) conditioned in acid solution

4. Discussion

An aminoalkylphosponate resin has three pKa values, two associated to -P-OH and one to amine (-NH_2-) functional groups. According to Fig. 7, acid behaviour is associated to the dissociation of the phosphonic acid functional groups whereas base properties are related to the secondary amino group. In the investigation of ion-exchange properties of aminophosphonate silica-based adsorbent, β-propylaminophosphonic acid was used as a model species and pKa values of 1.45, 5.31, and 11.0 were reported (Nesterenko et al., 1999). Therefore, the different species formed in solution as a function of pH are presented in Fig. 7. Forms II and III predominate under the experimental conditions of the current work (pH 4,0). Only one P-O^- group is available for bonding with Mn^{2+} ions in structure II, whereas two exchange groups (P-O^-) are present in structure III for the same molecule. Presumably, amine groups does not participate in the bonding process because $pK_{a,3}$ (11.0) is much higher than the value applied in the experiments(Nesterenko et al., 1999).

Resins with aminoalkylphosponate functional groups were developed for alkaline-earth cation uptake in concentrated brine solutions as separation factors as high as 21500 for the exchange of calcium for sodium were determined (Klipper et al., 1988). The resin selectivity for divalent cations (Cu, Ni, Zn,

Cd, Co, Ca) and also Na as compared to H^+ was investigated. Purolite S950 preferred protons to these metallic ions therefore metal uptake is improved at higher solution pH. In addition, Ca^{2+} had higher affinity for the resin as compared to Co^{2+}, Ni^{2+} and, as expected, Na^+ (Kiefer and Höll, 2001). Furthermore, another study proposed that this resin had higher affinity for Mn^{2+} in relation to Mg^{2+} (Perez et al., 2018), which is consistent with the results of the current work. An aminophosphonate-functionalized silca was synthetized to be applied in ionic chromatography and the bonding between metallic ions and the phosphonic group was speculated. The likely mode of chelation of metal ions by phosphonate groups comprises deprotonating of two P–OH groups. In addition, bonding to one of the hydroxyl groups and coordination with the oxygen atom in the P=O bond was also considered possible. Although several stoichiometries of metal complexes can be formed between the O, O chelating system of the ion exchanger and the metal cation, a 1:1 metal:ligand stoichiometry is considered the most stable species.

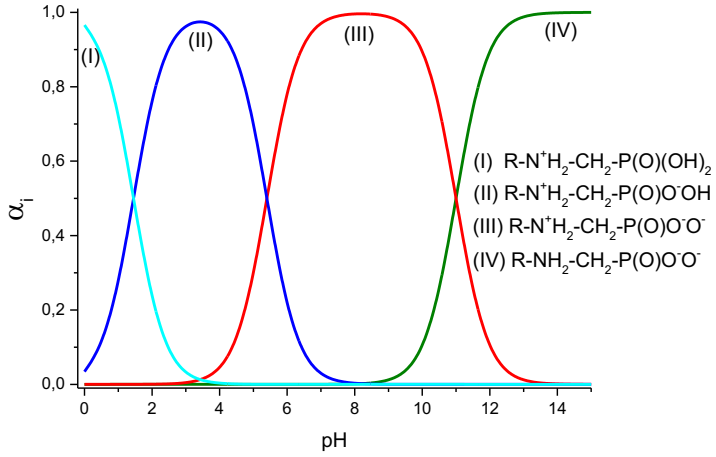

Fig. 7. Speciation diagram of β-propylaminophosphonic acid at 25°C and infinite dilution

Stability constants for metal-aminophosphonate complexes were determined in acid solutions for a series of metals including Mn^{2+}, Mg^{2+} and Ca^{2+} (Mohan and Abbott, 1978). The organic acids investigated were 1-aminoethylphosphonic, 2-aminoethylphosphonic and 2-amino-3-phosphono-propionic acids. Metal interactions with PO-OH groups at lower pH and PO-O$^-$ at higher pH values were investigated. In the case of Mn^{2+}, logK increased from 1.97 when the ligand was a PO-OH group to logK = 3.5 with PO-O$^-$. Similarly, logK also increased from 1.27 (PO-OH) to 1.84 (PO-O$^-$) in the case of Mg^{2+} and from 1.02 (PO-OH) to 1.43 (PO-O$^-$) with Ca^{2+}, highlighting the stronger interaction with the deprotonated phosphonate group. This justifies the higher affinity of Purolite S950 for Mn^{2+} ions at pH 4.5 revealed in Fig. 1. The constants reported by Mohan and Abbott (1978) however do not explain the negligible Mg^{2+} uptake observed in the current study and this requires further investigation.

The kinetic analysis carried out in the current study revealed that Mn^{2+} adsorption is described by the pseudo-second order model, similarly to several other studies, and with rate constant values varying from 0.0012g/mg·min (at 40°C) to 0.0017 g/mg·min (at 70°C). This is likely because the pseudo-second order equation can be applied to all loading data obtained throughout the entire test. On the other hand, the pseudo-first-order equation better describes the adsorption process while the total concentration of adsorption sites is much higher than the concentration of sites occupied by the species, i.e., at low metal loadings (Crini and Badot, 2008). A review on Mn^{2+} adsorption on different substrates showed that the magnitude of the rate constant is mostly found in the range 10^{-3} g/mg·min to 10^{-1} g/mg·min, regardless the adsorbent under investigation (Kapur and Mondal, 2016). In addition, adsorption of Mn^{2+} ions on the Purolite S950 chelating resin had an activation energy of 10.4 kJ/mol, as revealed in the current study. Surprisingly, the effect of temperature on the kinetics of Mn^{2+} adsorption, which enables the determination of the activation energy, is not extensively investigated). One of the few examples s is the adsorption of Mn^{2+} on the Sinco-430 cationic resin, which was also described by the pseudo-second order equation (k_2 = 0.049-0.068g/mg·min) and had an activation energy of 6.3kJ/mol (Zhuang et al., 2020). In addition, Mn^{2+} adsorption on a double Mn-Fe oxide (greensand) was also described by the second-order model with an activation energy of 12.9 kJ/mol, in the 25°C-45°C range. When zeolites

were applied as adsorbent, the kinetics of Mn^{2+} loading also followed the pseudo-second order equation (k_2 = 0.119g/mg·min), at pH 6.5, and the activation energy of the process was 55.6kcal/mol. This value was significantly lower than that observed by Rajic et al. (2009), 127.9kJ/mol, who investigated Mn^{2+} uptake by a natural zeolite in tests performed at pH 5.5. Activation energy values of up to 90 kJ/mol were determined for the diffusion of Zn^{2+} and Mg^{2+} ions in different zeolites (Dyer and Enamy, 1981; Dyer and Townsend, 1973) and thus the value determined in the current work is consistent with the pore-diffusion mechanism.

Several studies reported that the adsorption of Mn^{2+} ions on resins and zeolites is an endothermic process. Notwithstanding manganese loading on Purolite S950 had a standard enthalpy of -85.0 kJ/mol, implying in an exothermic process, similarly to what was proposed for the Mn^{2+} adsorption on graphene oxide (Suddai et al., 2017) and zeolite (Lin et al., 2020). In absolute terms, the adsorption of the Mn^{2+} ion on zeolites has a standard enthalpy of less than 40 kJ/mol, but values can be higher when adsorption occurs on manganese dioxide (+205.8 kJ/mol) (Camargo et al., 2019), and on chelating resins (current work), suggesting chemisorption on these two adsorbents. On the other hand, the entropy of Mn^{2+} adsorption in both resins and zeolites is usually positive, unlike the value determined herein and also when Mn^{2+} was adsorbed on graphene oxide (Suddai et al., 2017) and on a NaA zeolite (Lin et al., 2020). Positive values of entropy indicate an increase in the disorder of the system, which can be attributed to the release of water molecules from Mn^{2+} ions during adsorption (Eren et al., 2011). Additionally, negative values of entropy suggests a enthalpy-driven process, in which a decreased disorder at the interface implying in adsorbed ions to moving from the adsorbent to the liquid phase (Saha and Chowdhury, 2011).

The current work has successively demonstrated the applicability of the amino-phosphonic chelating ion exchange-resin Purolite S950 in the selective adsorption of Mn^{2+} in the presence of Ca^{2+} and Mg^{2+} ions when equimolar concentrations were studied. However, the Ca/Mn and Mg/Mn ratios in actual mine waters can vary substantially. Therefore, future work will focus on the application of chelating resins to these real effluents and also on columns experiments to further advance the process development.

5. Conclusions

Both Purolite S950 and C104E resins presented higher affinities for Mn^{2+} as compared to Ca^{2+} and Mg^{2+}, whereas Purolite C100 resin showed greater affinity for calcium in relation to manganese and magnesium. However, the results indicated that Purolite S950 is recommended to be applied in the removal of Mn^{2+} ions due to a high metal uptake (37.9 mg/mL-resin or 0.69 mmol/mL-resin) as compared to Ca^{2+} (3.2 mg/mL-resin or 0.08 mmol/mL-resin) and Mg^{2+} (~0 mg/mL-resin). Therefore, Purolite S950 is particularly suited to be applied in the treatment of neutral mine waters with high Mg/Mn ratios. In the case of Ca^{2+}, it was observed a small affinity for the metal and an efficient Mn^{2+} removal will depend on the Ca/Mn ratio of the mine water to be treated. Subsequent studies with Purolite S950 revealed that the kinetics of Mn^{2+} adsorption is described by the pseudo-second order model and is a pore-diffusion-controlled process with an activation energy of 6.42kJ/mol. In addition, Mn^{2+} adsorption on Purolite S950 is exothermic (ΔH^o = - 85.0 kJ/mol) and the negative standard entropy (ΔS^o = -274 J/mol·K) was attributed to the release of water molecules from Mn^{2+} ions during adsorption.

Acknowledgment

This study was sponsored by Conselho Nacional de Pesquisa e Desenvolvimento (CNPq), Fundação de Amparo à Pesquisa do Estado de Minas Gerais (FAPEMIG), Financiadora de Estudos e Projetos (FINEP), Coordenação de Aperfeiçoamento de Pessoal do Ensino Superior (CAPES) and Universidade Federal de Ouro Preto. The CAPES and CNPq scholarships to B. P. Amengol and V. A. Leão, respectively, are particularly acknowledged.

References

ADIANSYAH, J. S.; ROSANO, M.; VINK, S.; KEIR, G. 2015. *A framework for a sustainable approach to mine tailings management: disposal strategies.* J. Clean. Prod., 108 1050-1062.

AMENGOL, B. P. C. *Estudo cinético e termodinâmico da adsorção do manganês em resinas de troca iônica*. 2021. 68 f. Dissertação de mestrado - Programa de Pós-Graduação em Engenharia Ambiental, Universidade Federal de Ouro Preto.

BARBOZA, N. R.; GUERRA-SÁ, R.; LEÃO, V. A. 2016. *Mechanisms of manganese bioremediation by microbes: an overview.* J Chem Technol Biot, 91 (11), 2733-2739.

CAMARGO, F. C. F.; SILVA, G. d. L. C.; DE LEUCAS, H. L. B.; DE VASCONCELOS, M. R. *et al.* 2019. *Chemical and biological approach to remove Mn from aqueous solution.* Environ. Technol. Innov.. 15 100398.

COŞKUN, G.; ŞIMŞEK, İ.; ARAR, Ö.; YÜKSEL, Ü. *et al.* 2016. *Comparison of chelating ligands on manganese (II) removal from aqueous solution.* Desalin Water Treat, 57 (53), 25739-25746. DOI: 10.1080/19443994.2016.1153984.

CRINI, G.; BADOT, P.-M. 2008. *Application of chitosan, a natural aminopolysaccharide, for dye removal from aqueous solutions by adsorption processes using batch studies: A review of recent literature.* Prog. Polym. Sci., 33 (4), 399-447.

DYER, A.; ENAMY, H. 1981. *Mobility of magnesium ions in the synthetic zeolites A, X and 2.62-Y.* Zeolites, 1 (1), 7-10.

DYER, A.; TOWNSEND, R. P. 1973. *The mobility of cations in synthetic zeolites with the faujasite framework — V: The self-diffusion of zinc into X and Y zeolites.* J Inorg Nucl Chem, 35 (8), 3001-3008.

EL-AASSAR, M. R.; MOHAMED, F. M. 2021. *Characterization valorized anthracite and its application in manganese (VII) adsorption from aqueous solution; batch and column studies.* Micropor Mesopor Mat, 310 110641.

EREN, E.; GUMUS, H.; SARIHAN, A. 2011. *Synthesis, structural characterization and Pb(II) adsorption behavior of K- and H-birnessite samples.* Desalination, 279 (1), 75-85.

FIGUEIREDO, R. S.; SAMIR S. LEAO; LEÃO, V. A. 2018. *Cinética de adsorção de manganês em zeólitas exauridas.* Tecnol Metal Mater Min, 15 (1), 8-14.

GEMICI, B. T.; OZEL, H. U.; OZEL, H. B. 2021. *Removal of methylene blue onto forest wastes: Adsorption isotherms, kinetics and thermodynamic analysis.* Environ. Technol. Innov. 22 101501.

HADADI, V. 2020. *Synthesizing "sulfonated styrene-divinylbenzene polymer/Fe" nanocomposite for adsorption of Mn (II) and Zn (II) ions from the waste of alkaline battery recycling factories: kinetic, thermodynamic, and isotherm adsorption studies.* Polymer, 100 266-273

HAMABE, Y.; HIRASHIMA, Y.; IZUMI, J.; YAMABE, K. *et al.* 2009. *Properties of a bifunctional chelating resin containing aminomethylphosphonate and sulfonate derived from poly(ω-bromobutylstyrene-co-divinylbenzene) beads.* React. Funct. Polym., 69 (11), 828-835.

HEIKKINEN, P. M.; RÄISÄNEN, M. L.; JOHNSON, R. H. 2009. *Geochemical Characterisation of Seepage and Drainage Water Quality from Two Sulphide Mine Tailings Impoundments: Acid Mine Drainage versus Neutral Mine Drainage.* Mine Water Environ., 28 (1), 30-49

INSTITUTO MINEIRO DE GESTÃO DAS ÁGUAS. *Acompanhamento da qualidade das águas do rio doce após o rompimento da barragem da samarco no distrito de Bento Rodrigues – Mariana/MG.* Belo Horizonte, p. 49. 2015.

INSTITUTO MINEIRO DE GESTÃO DAS ÁGUAS. *Encarte especial sobre a qualidade das águas do rio doce após 5 anos do rompimento dambarragem de Fundão.* Instituto Mineiro de Gestão das Águas. Belo Horizonte, p. 74. 2020.

KAPUR, M.; MONDAL, M. K. 2016. *Design and model parameters estimation for fixed–bed column adsorption of Cu(II) and Ni(II) ions using magnetized saw dust.* Desalin Water Treat, 57 (26), 12192-12203.

KARTHIKEYAN, T.; RAJGOPAL, S.; MIRANDA, L. R. 2005. *Chromium(VI) adsorption from aqueous solution by Hevea Brasilinesis sawdust activated carbon.* J. Hazard. Mater., 124 (1–3), 192-199.

KIEFER, R.; HÖLL, W. H. 2001. *Sorption of Heavy Metals onto Selective Ion-Exchange Resins with Aminophosphonate Functional Groups.* Ind. Eng. Chem. Res., 40 (21), 4570-4576. DOI: 10.1021/ie010182l.

KLIPPER, R. M.; HOFFMANN, H.; MITSCHKER, A.; WAGNER, R. *Ion Exchange for Industry*. 1988. 243 p.

LEVENSPIEL, O. *Chemical reaction engineering*. 1 ed. New York: John Wiley & Sons, 1962. 578 p.

LIN, Z.; YUAN, P.; YUE, Y.; BAI, Z. *et al.* 2020. *Selective adsorption of Co(II)/Mn(II) by zeolites from purified terephthalic acid wastewater containing dissolved aromatic organic compounds and metal ions.* Sci Total Environ, 698 134287.

MARCU, C.; VARODI, C.; BALLA, A. 2021. *Adsorption Kinetics of Chromium (VI) from Aqueous Solution Using an Anion Exchange Resin.* Anal. Lett., 54 (1-2), 140-149.

MCCABE, W. L.; SMITH, J. C.; HARRIOTT, P. *Unit operations of chemical engineering*. 7 ed. New York: McGraw-Hill´s Science, 2005. Chemical Engineering Series.

MOHAN, M. S.; ABBOTT, E. H. 1978. *Metal complexes of biologically occurring aminophosphonic acids.* J. Coord. Chem., 8 (3), 175-182.

MORGAN, J. J. 2005. *Kinetics of reaction between O_2 and Mn(II) species in aqueous solutions.* Geochim. Cosmochim. Acta, 69 (1), 35-48.

NAZARIAN, R.; DESCH, R. J.; THIEL, S. W. 2021. *Kinetics and equilibrium adsorption of phosphate on lanthanum oxide supported on activated carbon*. Colloids Surf. A., 624 126813.

NESTEREKO, P. N.; SHAW, M. J.; HILL, S. J.; JONES, P. 1999. *Aminophosphonate-Functionalized Silica: A Versatile Chromatographic Stationary Phase for High-Performance Chelation Ion Chromatography*. Microchem. J., 62 (1), 58-69.

OWEN, J. R.; KEMP, D.; LÈBRE, É.; SVOBODOVA, K. *et al.* 2020. *Catastrophic tailings dam failures and disaster risk disclosure.* Int. J. Disaster Risk Reduct., 42 101361.

PEREZ, I. D.; CORREA, M. M. J.; TENÓRIO, J. A. S.; ESPINOSA, D. C. R. *Effect of the pH on the Recovery of Al^{3+}, Co^{2+}, Cr^{3+}, Cu^{2+}, Fe^{3+}, Mg^{2+}, Mn^{2+}, Ni^{2+} and Zn^{2+} by Purolite S950*. *In*: Energy Technology 2018, 2018, Springer International Publishing, p. 385-393.

RAJIC, N.; STOJAKOVIC, D.; JEVTIC, S.; ZABUKOVEC LOGAR, N. *et al.* 2009. *Removal of aqueous manganese using the natural zeolitic tuff from the Vranjska Banja deposit in Serbia.* J. Hazard. Mater., 172 (2), 1450-1457.

SAHA, P.; CHOWDHURY, S. Insight into adsorption thermodynamics. *In*: MIZUTANI, T. (Ed.). Thermodynamics, 2011. v. 16, p. 349-364.

SICUPIRA, D. C.; SILVA, T. T.; LEÃO, V. A.; MANSUR, M. B. 2014. *Batch removal of manganese from acid mine drainage using bone char.* Braz J Chem Eng, 31 195-204.

SRACEK, O.; FILIP, J.; MIHALJEVIČ, M.; KŘÍBEK, B. *et al.* 2011. *Attenuation of dissolved metals in neutral mine drainage in the Zambian Copperbelt.* Environmental Monitoring and Assessment, 172 (1), 287-299.

SUDDAI, A.; NUENGMATCHA, P.; CHANTHAI, S. 2017. *Adsorptive removal of manganese (II) from aqueous solution using graphene oxide: A kinetics and thermodynamics study.* Orient. J. Chem., 33 (4), 1899-1904.

TUCK, C. C. *Iron ore.* National Minerals Information Center, p. 2. 2020.

WU, Y.; LI, B.; FENG, S.; MI, X. *et al.* 2009. *Adsorption of Cr(VI) and As(III) on coaly activated carbon in single and binary systems.* Desalination, 249 (3), 1067-1073

ZHUANG, H.; ZHONG, Y.; YANG, L. 2020. *Adsorption equilibrium and kinetics studies of divalent manganese from phosphoric acid solution by using cationic exchange resin.* Chinese J Chem Eng, 28 (11), 2758-2770.